Available online at www.sciencedirect.com

SciVerse ScienceDirect

Ceramics International 39 (2013) 2645–2650

CERAMICS INTERNATIONAL

www.elsevier.com/locate/ceramint

Nanocrystalline $BaAl_2O_4$ powders prepared by aqueous combustion synthesis

Robert Ianoş*, Radu Lazău, Roxana Băbuţă, Silvana Borcănescu, Cristian Renato Boruntea

"Politehnica" University of Timisoara, Faculty of Industrial Chemistry and Environmental Engineering, P-ţa Victoriei no. 2, Timişoara 300006, Romania

Received 30 July 2012; received in revised form 1 August 2012; accepted 9 September 2012
Available online 18 September 2012

Abstract

In order to achieve $BaAl_2O_4$ formation via combustion synthesis, two types of recipes were designed: single fuel recipes (urea, glycine, β-alanine or hexamethylenetetramine) and innovative fuel mixture recipes (urea + glycine, urea + β-alanine and urea + hexamethylenetetramine respectively). No combustion reactions were noticed in the case of single fuel recipes based on urea or hexamethylenetetramine. The only crystalline phase present in the case of the powders obtained in such a way was unreacted $Ba(NO_3)_2$. Glycine and β-alanine generated smoldering reactions, leading to the formation of black powders, which consist of $Ba(NO_3)_2$, $BaCO_3$ and traces of $BaAl_2O_4$ (in the case of β-alanine). Fuel mixture recipes proved to be better than single fuel recipes, yielding $BaAl_2O_4$ as main crystalline phase. The specific surface area of the resulted powders ranges between 2.0 and 3.9 m^2/g. The urea and glycine fuel mixture was the most efficient yielding $BaAl_2O_4$ with an average crystallite size of 60 nm.

Keywords: A. Powders: chemical preparation; D. Alkaline earth oxides; Barium aluminate

1. Introduction

Barium aluminates are important materials with applications in various fields, such as refractory cements, catalysts, humidity sensors and especially phosphor materials with high initial luminescence intensity, long afterglow and chemical stability [1–6].

The first compound to be discovered in the $BaO–Al_2O_3$ system was $BaAl_2O_4$ (barium monoaluminate), which is a member of the compact trydimite tetrahedral structure [7,8]. Other well-known compounds in the system are $3BaO \cdot Al_2O_3$, $BaO \cdot 4Al_2O_3$ and $BaO \cdot 6Al_2O_3$ [9–11].

Various methods have been tested for the preparation of $BaAl_2O_4$ powders. For instance, Zaki et al. [9] obtained barium monoaluminate as major crystalline phase using the ceramic method, after annealing a mechanical mixture of α-Al_2O_3 and $BaCO_3$ at 1200 °C for 2 h.

One of the most frequently used synthesis method is based on the annealing of the precursors resulted from sol–gel process [12–14]. Other methods reported in the literature include mechano-chemical route [15], wet chemical conversion route [16], hydrothermal precipitation–calcination route [17], self-propagating high temperature synthesis [18] or solution combustion synthesis [19–21].

In this context, the paper is aimed on obtaining nanocrystalline $BaAl_2O_4$ directly from the combustion reaction, using fuel mixtures as a novel alternative to the less efficient single fuel approach.

2. Experimental procedure

2.1. Preparation of ceramic powders

The starting raw materials used in all experiments were pro analysi reagents. Molar compositions of the investigated samples are shown in Table 1. Samples 1–4 correspond to stoichiometric metal nitrates – single fuel recipes, using urea, glycine, β-alanine, and hexamethylenetetramine as fuels. Samples 5–7 are novel stoichiometric recipes, since they involve the use of two fuel mixtures (urea + glycine, urea + β-alanine, urea + hexamethylenetetramine).

*Corresponding author. Fax: 0040 403060.
E-mail address: robert_Ianos@yahoo.com (R. Ianoş).

0272-8842/$ - see front matter © 2012 Elsevier Ltd and Techna Group S.r.l. All rights reserved.
http://dx.doi.org/10.1016/j.ceramint.2012.09.030

Table 1
Molar ratio of the investigated samples.

No.	Oxidizing agents		Reducing agents (fuels)			
	$Ba(NO_3)_2$, Merck p.a.	$Al(NO_3)_3 \cdot 9H_2O$ Merck p.a.	CH_4N_2O, Merck p.a.	$C_2H_5NO_2$, Fluka p.a.	β-$C_3H_7NO_2$, Merck p.a.	$C_6H_{12}N_4$, Reactivul p.a.
1.	3	6	20	–	–	–
2.	9	18	–	40	–	–
3.	3	6	–	–	8	–
4.	9	18	–	–	–	10
5.	9	18	45	10	–	–
6.	3	6	15	–	2	–
7.	18	36	90	–	–	5

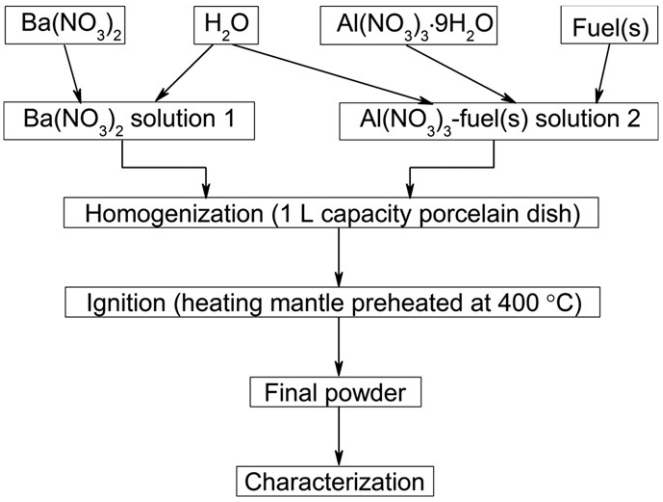

Fig. 1. Flowchart of the aqueous combustion synthesis of $BaAl_2O_4$ powders.

Recipes were calculated for a yield of 0.03 mol of $BaAl_2O_4$, assuming the reaction by-products are H_2O, CO_2 and N_2.

Fig. 1 shows the preparation scheme of $BaAl_2O_4$ powders via aqueous combustion synthesis. The appropriate amount of barium nitrate was dissolved in 40 mL of distilled water at 70 °C (solution 1). The required amount of aluminum nitrate and fuel(s) were dissolved in 10 mL of distilled water at 50 °C (solution 2).

After the complete dissolution of raw materials, the two clear solutions (1 and 2) were mixed in a porcelain evaporating dish. Due to its low solubility, some of the barium nitrate precipitates from the solution. Ignition of the combustion reactions was done by placing the porcelain dish in a heating mantle, preheated at 400 °C.

As the temperature of the precursor increased, a self-propagating combustion reaction occurred (except for samples 1 and 4), leading to the formation of a fluffy material. Digital video recordings of the combustion reactions were used to estimate the time span between the ignition of the combustion reactions and their completion. The fluffy material resulted at the end of the combustion process was hand-crushed with a pestle. Small portions of each sample were annealed for 1 h at 900 °C in order to determine the loss on ignition.

2.2. Characterization techniques

The phase composition of the powders was established by X-ray diffraction, using a Rigaku Ultima IV diffractometer operating at 40 kV and 40 mA. The X-ray diffraction patterns were recorded using the Ni filtered $Cu_{K\alpha}$ radiation. Crystallite size and lattice parameters were calculated using the whole pattern profile fitting method (WPPF) and PDXL2 software.

Heating behavior of the combustion synthesized powders was monitored by thermal analysis using a Netzsch STA 449 C instrument equipped with Pt crucibles. The TG curves were recorded under artificial air flow of 20 mL/min, over the interval 25–900 °C at a heating rate of 10 °C/min. BET specific surface area of the powders was measured by $N_{2(g)}$ adsorption technique using a Micromeritics ASAP 2020 instrument. Particle morphology was investigated by SEM, using a FEI Inspect S scanning electron microscope.

3. Results and discussion

3.1. Observations on the combustion reactions

Analyzing the combustion reactions one may notice the way the reaction evolves in the case of single fuel recipes 1–4 highly depends on the used fuel (Fig. 2). Urea and hexamethylenetetramine are not capable of producing self-propagated combustion reactions. A high amount of gases evolves but the samples do not reach incandescence and the combustion front cannot be distinguished. In the case of sample 4, prepared with hexamethylenetetramine, the gas evolving does not last as long as in the case of sample 1 prepared with urea.

In the case of samples 2 and 3 prepared with glycine and β-alanine, the reactions evolve in a self-propagated manner. As soon as the combustion reaction is ignited, the combustion front spans across the raw material mixture leading to a black reaction product containing residual carbon. These experimental findings question the efficiency of using a single fuel for the preparation of $BaAl_2O_4$ via combustion synthesis.

Considering the above mentioned findings and also the literature data [22–24] suggesting that there is a predilection of metal nitrates with respect to certain fuels, a new approach has been suggested: using fuel mixtures instead of a single fuel. Basically, in the case of fuel mixture recipes the assumption was made that urea will react with $Al(NO_3)_3$ whilst glycine, β-alanine or hexamethylenetetramine will react with $Ba(NO_3)_2$.

The combustion reactions of the samples prepared with fuel mixtures (samples 5–7) stand out by a much shorter duration of the redox processes (Fig. 2) and also by a stronger incandescence of the combustion front. The images captured during the combustion reactions (Fig. 3) in the case of samples 2 (single fuel – glycine) and 5 (urea and glycine fuel mixture) highlight the different incandescence and exothermicity developed in the two approaches.

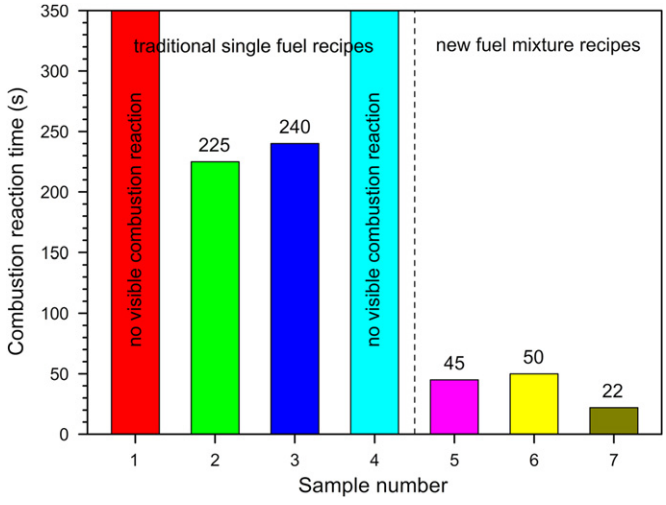

Fig. 2. Combustion reaction time determined based on the digital video recordings.

The fact that fuel mixture recipes generate more exothermic redox reactions than the conventional single fuel recipes increases the chances of obtaining $BaAl_2O_4$ directly from the combustion reaction, with no additional annealing being required.

Fig. 4 shows the images of the powders 1–7 prepared by combustion synthesis, after manual grinding. The powders obtained with a single fuel have colors varying from white to yellowish and black. On the other hand, fuel mixture recipes lead to white or gray powders.

3.2. XRD characterization

XRD patterns of powders 1–7 resulted from the combustion process are presented in Fig. 5. The phase composition can be very well correlated to the evolution of the reactions. $Ba(NO_3)_2$ is the only crystalline phase present on the diffraction patterns of samples 1 and 4 (single fuel recipes), where no visible combustion reaction occurred.

It is worth mentioning that other authors [19,21] who had used urea as fuel also reported the presence of $Ba(NO_3)_2$ in the reaction product. The XRD pattern of sample 3 indicates the presence of $BaCO_3$ alongside with very small amounts of $Ba(NO_3)_2$ and $BaAl_2O_4$. Sample 2 contains mainly unreacted $Ba(NO_3)_2$ and traces of $BaCO_3$.

The presence of $Ba(NO_3)_2$ in all the samples prepared with a single fuel shows that no combustion reactions have actually taken place in the case of samples 1 and 4, and also confirms the low exothermicity of the combustion reactions in the case of samples 2 and 3. The formation of $BaCO_3$ in samples 2 and 3 may be explained by the presence of CO_2 in the combustion generated gases, corroborated with the relatively low temperature reached during the combustion process. The absence of $BaAl_2O_4$

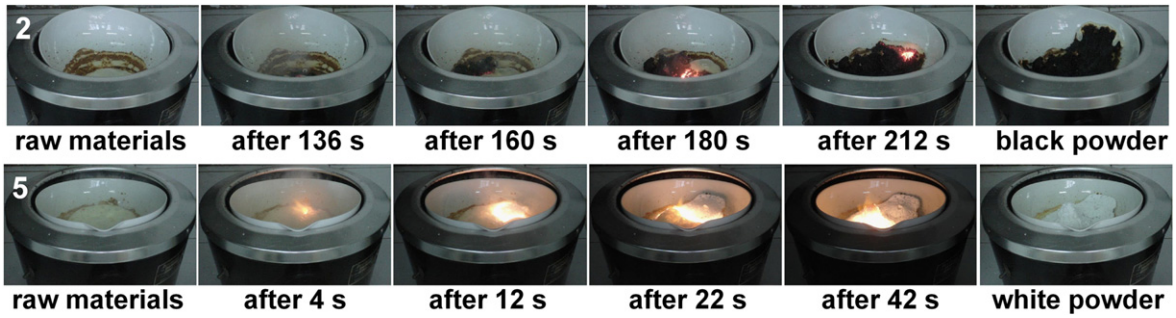

Fig. 3. Relevant image sequence during the evolution of combustion reactions (samples 2 and 5).

Fig. 4. Photographic images of samples 1–7 after manual grinding.

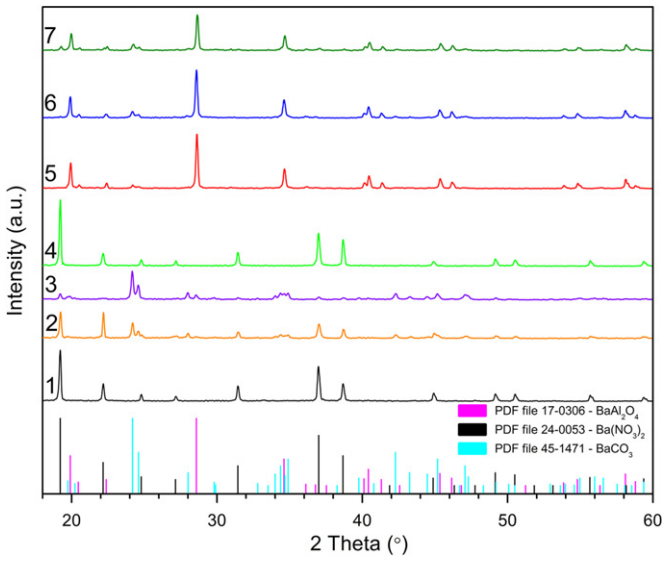

Fig. 5. XRD patterns of samples 1–7 prepared by combustion synthesis.

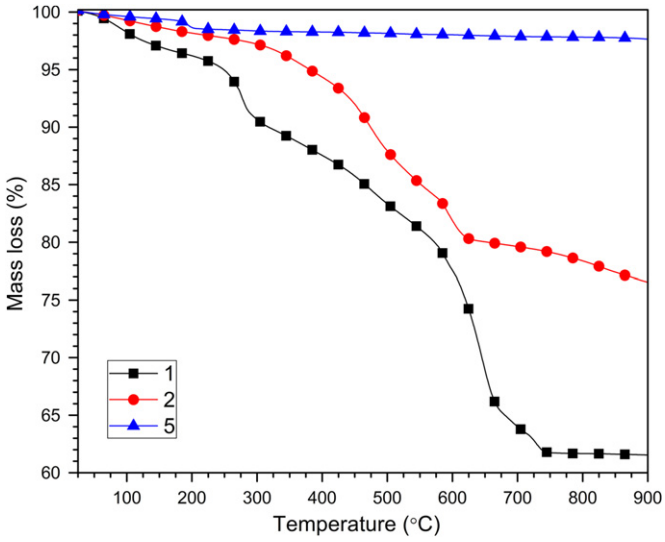

Fig. 6. TG curves of powders 1, 2 and 5, prepared by combustion synthesis.

Table 2
Crystallite size, lattice parameters and BET surface area of powders 5–7.

No.	D [nm]	a [Å]	c [Å]	S_{BET} [m^2/g]
5.	60	10.450	8.789	2.0
6.	50	10.448	8.795	3.9
7.	54	10.450	8.793	2.2

from samples 1, 2 and 4, as well as the presence of very small amounts of $BaAl_2O_4$ in sample 3 indicates that the temperature developed within the raw material mixture was not high enough.

On the other hand, combustion reactions involving the use of fuel mixtures (samples 5–7) are highly exothermic, which makes $BaAl_2O_4$ the main crystalline phase present on the XRD patterns (Fig. 5). The phase composition of sample 5 consists of single phase $BaAl_2O_4$, with an average crystallite size of 60 nm (Table 2). Obtaining $BaAl_2O_4$ crystallites of this size may prove to be very useful in the synthesis of phosphor materials, where the overall properties and especially the afterglow period are positively influenced by the large crystallite size.

In the case of samples 6 and 7, $BaCO_3$ and even $Ba(NO_3)_2$ traces (sample 7) could be noticed on the XRD patterns alongside $BaAl_2O_4$. This indicates a lower combustion temperature than in the case of sample 5, which is also confirmed by the lower crystallite size in the case of samples 6 and 7 (Table 2). At the same time, the specific surface of samples 6 and 7 are higher than that in the case of sample 5. $BaAl_2O_4$ crystallite size varies between 50 and 60 nm and the calculated cell parameters are very close to those mentioned in the PDF file 17–0306 ($a=b=10.44$ Å, $c=8.794$ Å).

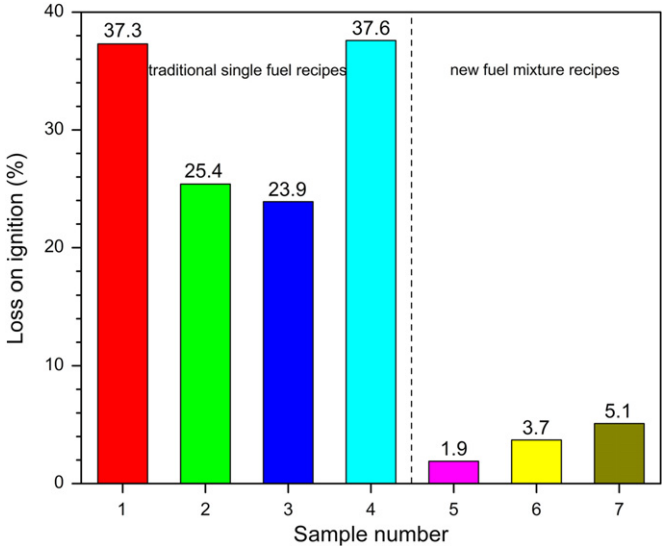

Fig. 7. Loss on ignition of samples 1–7 prepared by combustion synthesis.

3.3. Thermal analysis investigations

Thermal analysis represents a very efficient method to assess the degree of completion in the case of combustion reactions, by performing the analysis on the powders resulted from the combustion itself. In an ideal situation, $BaAl_2O_4$ would form directly from the combustion reaction and the mass of the sample subjected to heating should be constant, which translates into a mass versus temperature variation represented by a horizontal straight line.

In reality, the actual shape of the TG curves of samples 1 and 2 (Fig. 6) suggests the development of further processes accompanied by a significant mass loss: 38.5%

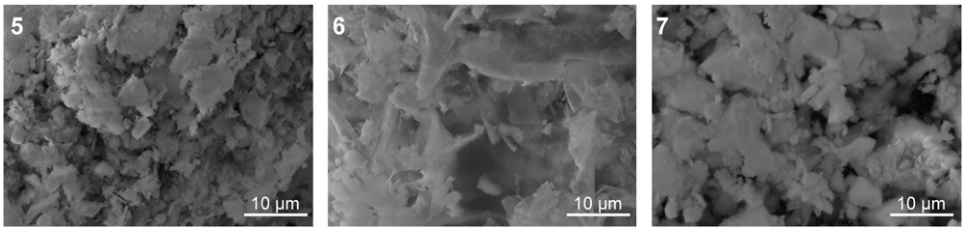

Fig. 8. SEM images of samples 5–7 prepared by combustion synthesis.

for sample 1 and 23.5% for sample 2. The higher mass loss in the case of sample 1 is in accordance with the reaction development: no visible combustion reaction was noticed in the case of sample 1 prepared with urea, whilst a smoldered reaction was noticed in the case of sample 2 prepared with glycine.

The mass loss of samples 1 and 2 may be assigned on one hand, to the $Ba(NO_3)_2$ and $BaCO_3$ decomposition (these phases have already been confirmed by XRD, Fig. 5) and on the other hand, to the removal of the organic residue originating from the used fuel.

Sample 5 (prepared with a mixture of urea and glycine) presents 2.4% mass loss, which suggests a much more energetic development of the combustion reaction, compared with samples 1 and 2. Moreover, one may notice that this mass loss mainly takes place below 200 °C.

Fig. 7 shows the loss on ignition of samples 1–7 determined by annealing the initial powders at 900 °C for 1 h. It should be noted that there is an excellent agreement between the mass loss of samples 1, 2 and 5 determined by thermal analysis and the loss on ignition of the samples.

The samples obtained with a single fuel (1–4) present over 23% loss on ignition, which is in accordance with the observations concerning the reactions development and the XRD results. Since no combustion reactions were noticed in the case of samples 1 and 4, these powders exhibit the highest loss on ignition, over 37%. Samples 2 and 3 resulted from smoldering combustion reactions, therefore they present a lower loss on ignition than samples 1 and 4.

The samples prepared with fuel mixtures (5–7) show much lower losses on ignition (below 6%), which confirm once again that fuel mixture recipes are able to generate higher combustion temperature than single fuel recipes. Sample 5, where $BaAl_2O_4$ is the single crystalline phase, presents the lowest loss on ignition. Samples 6 and 7 show slightly higher losses on ignition due to the presence of $BaCO_3$ and $Ba(NO_3)_2$ traces (Fig. 5).

3.4. SEM characterization

The SEM images of the powders 5–7 indicate that the particles have an irregular shape and are strongly agglomerated, independently of the used fuel mixture (Fig. 8). This is a consequence of the large volume of gases evolving during the combustion reactions and the high temperature obtained within the reaction mixture, which enhances $BaAl_2O_4$ formation and particle agglomeration in microstructures with size below 10 μm.

4. Conclusions

Two types of recipes were used in order to obtain $BaAl_2O_4$ via combustion synthesis:

- single fuel recipes (urea, glycine, β-alanine and hexamethylenetetramine);
- new fuel mixture recipes (urea + glycine, urea + β-alanine, urea + hexamethylenetetramine).

The classical single fuel recipes did not yield pure $BaAl_2O_4$ directly from the combustion reaction; in fact, no typical combustion reaction was noticed at all in the case of the recipes using urea and hexamethylenetetramine as single fuels. The only crystalline phase evidenced on the XRD patterns of the samples obtained in such a way was $Ba(NO_3)_2$. Glycine and β-alanine generated smoldering combustion reactions leading to black powders. The phase analysis of these powders showed the presence of $Ba(NO_3)_2$, $BaCO_3$ and traces of $BaAl_2O_4$ (in the case of β-alanine recipe).

The innovative fuel mixture approach proved to be superior to the traditional single fuel approach and yielded $BaAl_2O_4$ as the main crystalline phase. The resulted powders have a specific surface area varying between 2.0 and 3.9 m^2/g. Urea and glycine fuel mixture was the most efficient and yielded single phase $BaAl_2O_4$, with a crystallite size of 60 nm. Traces of $BaCO_3$ and even $Ba(NO_3)_2$ were still found in the case of recipes using urea + β-alanine and urea + hexamethylenetetramine fuel mixtures.

Acknowledgments

This work was supported by a grant of the Romanian National Authority for Scientific Research, CNCS – UEFISCDI, project number PN-II-RU-TE-2011-3-0024 (18/05.10.2011). Authors would also like to acknowledge Paula Sfîrloagă (National Research Institute for Electrochemistry and Condensed Matter, Timisoara, Romania) for performing the SEM investigations.

References

[1] M.R. Rezaie, H.R. Rezaie, R. Naghizadeh, The effect of SiO_2 additions on barium aluminate cement formation and properties, Ceramics International 35 (2009) 2235–2240.

[2] M. Casapu, J.D. Grunwaldt, M. Maciejewski, M. Wittrock, U. Göbel, A. Baiker, Formation and stability of barium aluminate and cerate in NO*x* storage-reduction catalysts, Applied Catalysis B—Environmental 63 (2006) 232–242.

[3] J.J. Vijaya, L.J. Kennedy, G. Sekaran, K.S. Nagaraja, Synthesis, characterization and humidity sensing properties of Sr(II)-added $BaAl_2O_4$ composites, Sensors and Actuators B—Chemical 124 (2007) 542–548.

[4] S.Y. Raghvendra, S.K. Pandey, A.C. Pandey, $BaAl_{12}O_{19}$: Mn^{2+} green emitting nanophosphor for PDP application synthesized by solution combustion method and its vacuum ultra-violet photoluminescence characteristics, Journal of Luminescence 131 (2011) 1998–2003.

[5] V. Singh, V. Natarajan, J.J. Zhu, Studies on Eu doped Ba and Zn aluminate phosphors prepared by combustion synthesis, Optical Materials 29 (2007) 1447–1451.

[6] Z. Qiu, Y. Zhou, M. Lü, A. Zhang, Q. Ma, Combustion synthesis of long-persistent luminescent MAl_2O_4: Eu^{2+}, R^{3+} (M=Sr, Ba, Ca, R=Dy, Nd and La) nanoparticle and luminescence mechanism research, Acta Materialia 55 (2007) 2615–2620.

[7] V.H. Wartenberg, H.J. Reusch, Melting diagrams of refractory oxides, Journal of Inorganic and General Chemistry 207 (1932) 1–20.

[8] A.K. Larsson, R.L. Withers, J.M. Perez-Mato, J.D. Fitzgerald, P.J. Saines, B.J. Kennedy, Y. Liu, On the microstructure and symmetry of apparently hexagonal $BaAl_2O_4$, Journal of Solid State Chemistry 181 (2008) 1816–1823.

[9] M.I. Zaki, G.A.M. Hussien, R.B. Fahim, Characterization of the powder mixture of the reaction between alumina and barium carbonate, Journal of Materials Science Letters 4 (1985) 517–522.

[10] L. Perier-Camby, A.M. Vernay, T. Gregory, Solid way synthesis of barium aluminate. High temperature X-ray diffraction study of intermediary compounds, Materials Science Forum 79–82 (1991) 671–680.

[11] L. Perier-Camby, T. Gregor, Chemical reaction for preparation of $BaAl_2O_4$; study of reaction kinetics and mechanism, Journal de Chimie Physique et de Physico-Chimie Biologique 91 (1994) 1763–1773.

[12] W.A. Al-Douri, M. Biedermann, Q.G. Chen, T.J. Davis, H.G. Emblem, Refractory oxides containing Ba and Al, European Journal of Solid State and Inorganic Chemistry 33 (1996) 507–518.

[13] C. Zhang, L. Wang, L. Cui, Y. Zhu, A novel method for the synthesis of nano-sized $BaAl_2O_4$ with thermal stability, Journal of Crystal Growth 255 (2003) 317–323.

[14] M. Giannos, M. Hoang, W.T. Turney, Thermally stable aluminas for high-temperature applications, Chemistry Letters 27 (1998) 793–794.

[15] T.F. Grigorieva, A.P. Barinova, E.Y. Ivanov, V.V. Boldyrev, Mechanochemical synthesis of nanocrystal complex oxides, Russian Journal of Physical Chemistry 354 (1997) 489–492.

[16] P. Padmini, T.R. Narayan, Wet chemical synthesis of ultrafine multicomponent ceramic powder through gel to crystallite conversion, Journal of Materials Chemistry 4 (1994) 1875–1881.

[17] D. Mishra, S. Anand, R.K. Panda, D.R. Prasad, Characterization of products obtained during formation of barium monoaluminate through hydrothermal precipitation–calcination route, Journal of the American Ceramic Society 85 (2002) 437–443.

[18] T. Sathaporn, S. Niyomwas, Synthesis and characterization of MAl_2O4 (M=Ba, Ca, Sr) phosphor by self-propagating high temperature synthesis, Energy Procedia 9 (2011) 410–417.

[19] B.M. Mothudi, O.M. Ntwaeaborwa, J.R. Botha, H.C. Swart, Photoluminescence and phosphorescence properties of MAl_2O_4: Eu^{2+}, Dy^{3+} (M=Ca, Ba, Sr) phosphors prepared at an initiating combustion temperature of 500 °C, Physica B—Condensed Matter 404 (2009) 4440–4444.

[20] L.C.V. Rodrigues, R. Stefani, H.F. Brito, M.C.F.C. Felinto, J. Hölsä, M. Lastusaari, T. Laamanen, M. Malkamäki, Thermoluminescence and synchrotron radiation studies on the persistent luminescence of $BaAl_2O_4$: Eu^{2+}, Dy^{3+}, Journal of Solid State Chemistry 183 (2010) 2365–2371.

[21] F. Sun, J. Zhao, Blue-green $BaAl_2O_4$: Eu^{2+}, Dy^{3+} phosphors synthesized via combustion synthesis method assisted by microwave irradiation, Journal of Rare Earths 29 (2011) 326–329.

[22] R. Ianoș, I. Lazău, C. Păcurariu, Metal nitrate/fuel mixture reactivity and its influence on the solution combustion synthesis of γ-$LiAlO_2$, Journal of Thermal Analysis and Calorimetry 97 (2009) 209–214.

[23] R. Ianoș, I. Lazău, C. Păcurariu, P. Barvinschi, Fuel mixture approach for solution combustion synthesis of $Ca_3Al_2O_6$ powders, Cement and Concrete Research 39 (2009) 566–572.

[24] R. Ianoș, I. Lazău, C. Păcurariu, P. Barvinschi, Solution combustion synthesis of $MgAl_2O_4$ using fuel mixtures, Materials Research Bulletin 43 (2008) 3408–3415.